

# Supernova constraints on neutrino mass and mixing

Srubabati Goswami, Physical Research Laboratory, Ahmedabad 380009, INDIA

## Abstract

In this article I review the constraints on neutrino mass and mixing coming from type-II supernovae. The bounds obtained on these parameters from shock reheating, r-process nucleosynthesis and from SN1987A are discussed. Given the current constraints on neutrino mass and mixing the effect of oscillations of neutrinos from a nearby supernova explosion in future detectors will also be discussed.

## 1 Overview of type-II supernova

Massive stars with  $8M_{\odot} \leq M \leq 60M_{\odot}$  shine for  $10^7$  years via thermonuclear burning producing successively  $H, He, C, O$  and so on. The end product of this chain is  $^{56}Fe$ . Since  $Fe$  has the highest binding energy per nucleon the thermonuclear reactions stop at the center and the pressure ceases to have a part coming from radiation. At this stage the star has a “onion-skin” structure. As the mass of the core becomes greater than the Chandrasekhar limiting mass the pressure of the relativistic electron gas alone can no longer counterbalance the inward gravitational pressure. The collapse is triggered off by the photodissociation of  $Fe$ -nuclei and/or electron capture which reduces the electron gas pressure further. As the collapse proceeds the core density rises, causing an increase in the electron chemical potential. Subsequently the electron Fermi energy becomes higher than the capture threshold and facilitates electron capture by nuclei and free protons leading to the neutronization of the core. This further reduces the  $e^-$  pressure thereby accelerating the collapse. This is known as the infall stage [1]. When the core density becomes of the order of supranuclear densities ( $10^{14}g/cc$ ) the infall is halted and the infalling material bounces back. The outer core still continues its infall. The collision of this rebounding inner core with the infalling outer core re-

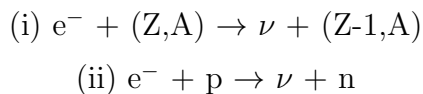
sults in the propagation of a shock wave into the mantle. This shock wave is believed to be instrumental in causing the supernova explosion. The inner core develops into the ‘proto-neutron star’.

## 1.1 Neutrino Production and Trapping

There are three distinct phases of neutrino emission from a type-II supernova.

- the infall phase
- the prompt  $\nu_e$  burst
- the thermal emission phase

During the infall stage, mainly electron neutrinos are produced via ‘neutronization’ reactions:



As positrons are much fewer, the corresponding antineutrinos cannot be produced by similar reactions. Also, since the  $\mu$  and  $\tau$  leptons present are negligible in number, charged current interactions leading to the production of  $\nu_\mu$  and  $\nu_\tau$  can be neglected. The thermal processes that yield  $\nu\bar{\nu}$  pairs of all flavors are largely suppressed while the infall proceeds, since the temperature is not high enough.

Initially these neutrinos escape freely from the star but subsequently the weak interaction of these neutrinos with nuclei and nucleons inhibits such free-streaming and neutrinos transport outwards by diffusion. The transport of neutrinos outwards has been considered using different detailed schemes [2]. A semianalytic approach adopted in [3]. uses neutrino diffusion equation,

$$\frac{\partial n_\nu}{\partial t} = \frac{1}{r^2} \frac{\partial}{\partial r} \left( r^2 \frac{1}{3} c \lambda_\nu \frac{\partial n_\nu}{\partial r} \right) \quad (1)$$

where  $\lambda_\nu$  is the neutrino mean free path given by [4]

$$\lambda_\nu = 1.0 \times 10^6 \rho_{12}^{-1} \left( \frac{1}{12} X_h \bar{A} + X_n \right)^{-1} \left( \frac{E_\nu}{10 \text{ MeV}} \right)^{-2} \text{ cm.} \quad (2)$$

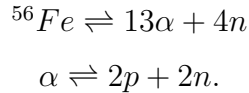
$X_h$  and  $X_n$  are the fractions by mass of heavy nuclei and neutrons.  $\rho_{12}$  is the density of stellar material in  $10^{12}$  g/cc. Using equation (1) it was shown that the neutrinos diffuse out of the material in about  $\frac{1}{9}$  sec. This is much larger than the hydrodynamic time scale of collapse which is of the order of 1 millisecond. This indicates that the  $\nu_L$ 's are effectively trapped within the core during the collapse.

Subsequently they are emitted from a “neutrino-sphere” which is defined as the radius from where the neutrinos can escape freely:

$$\int_{R_\nu}^{\infty} \frac{dr}{\lambda_\nu} = \frac{2}{3} \quad (3)$$

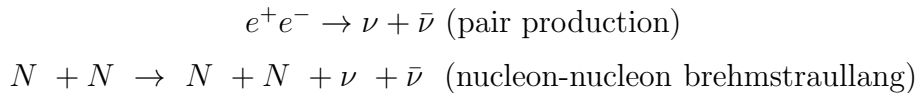
where  $\lambda_\nu$  is given by eq. (2).

The prompt  $\nu_e$  burst is emitted when the shock wave (being formed at a distance  $\sim 20$  km) passes through the neutrino-sphere (which is at a distance of  $\sim 50$  km at this epoch). The passage of the shock dissociates the  ${}^{56}\text{Fe}$  nuclei:



The neutrinos are produced via e capture on these protons causing this prompt  $\nu_e$  burst. However most of the neutrinos still remain trapped within the inner core.

In the shock heated regions, thermal processes produce  $\nu\bar{\nu}$  pairs.



Neutrinos and antineutrinos of all flavours are produced by these processes.

## 2 How does supernova explode?

For stars in the mass range  $8M_\odot \leq M \leq 15M_\odot$ , under some very special conditions on the size and structure of the core and the equation of state, the shock continues its

outward propagation and the star explodes within some tens of milliseconds after the beginning of collapse. This is the prompt explosion scenario [5]. For more massive stars the energy of the shock gets dissipated in dissociating nuclei and producing  $\nu\bar{\nu}$  pairs and the shock stalls at a radius of a few hundred kms and becomes an accretion shock. It is subsequently revived by the heating caused by neutrinos from the neutrino-sphere. This is the delayed explosion mechanism [6, 7]. However this mechanism generates a feeble shock with energies less than  $10^{51}$  ergs, a factor of 3 to 4 less than observed values.

Various mechanisms are considered which can generate a successful shock. It is now realised that convection of matter in the core plays a crucial role in the energy transport [8] and hydrodynamic calculations in two or three dimensions are being pursued by different groups [9]. Other important mechanisms like improved -supernova conditions, soft equation of state, general relativity at high densities, and improved neutrino physics have all been invoked to solve this problem. Fuller *et al.* [10] pointed out that matter-enhanced resonant flavor conversions of neutrinos in the region between the neutrino-sphere and the stalled shock can increase the shock heating rate appreciably and can result in a delayed explosion with energy  $\geq 10^{51}$  ergs, for a cosmologically significant  $\nu_\mu$  or  $\nu_\tau$  mass of 10 – 100 eV and small vacuum mixing angle. The basic idea is that due to neutrino flavor mixing  $\nu_{\mu S}$  or  $\nu_{\tau S}$  get converted to  $\nu_{e S}$ . Since  $\nu_\mu$  and  $\nu_\tau$  undergoes only neutral current interactions whereas  $\nu_e$  undergoes both neutral current and charged current interaction the average energy of  $\nu_\mu$  or  $\nu_\tau$  is higher than that of  $\nu_e$ . Thus the upshot of such flavor conversion is production of higher energy  $\nu_{e S}$  which can heat the shock more effectively. Since  $\nu_e$ 's are assumed to undergo MSW resonance the  $\bar{\nu}_{e S}$  remain unaffected.

The late time neutrino heating of the shock is caused by their absorption reactions on the nuclei as well as on free nucleons and by charged and neutral current scattering reactions. In this scenario the energy absorbed by matter behind the shock front/g/sec

assuming the matter to be nucleonic is given by [7],

$$\dot{E} = (223\text{MeV/nucleon sec}) \frac{1}{R_7^2} \left[ X_p L_{52}(\bar{\nu}_e) \left( \frac{T_{\bar{\nu}_e}}{5\text{MeV}} \right)^2 + X_n L_{52}(\nu_e) \left( \frac{T_{\nu_e}}{5\text{MeV}} \right)^2 \right] \quad (4)$$

where  $R_7$  is the radial distance from the center of the star units of  $10^7$  cm,  $L_{52}$  denotes the neutrino luminosity in units of  $10^{52}$  ergs/sec,  $X_n$  and  $X_p$  are the neutron and proton fractions respectively and  $T_{\nu_s}$  are the temperatures of the respective neutrino-spheres. In presence of complete flavour conversion between  $\nu_e$  and  $\nu_\tau$  the  $T_{\nu_e}$  in the above equation would be changed to  $T_{\nu_\tau}$ . One can make a rough estimate of the increase in heating rate assuming the luminosities to be equal when one obtains

$$\frac{\dot{E}_{\text{osc}}}{\dot{E}} = X_p + X_n \left( \frac{T_{\nu_\tau}}{T_{\bar{\nu}_e}} \right)^2. \quad (5)$$

Taking some typical values,  $T_{\nu_\tau} \approx 7$  MeV,  $T_{\bar{\nu}_e} \approx 5$  MeV,  $X_n \approx 2/3$  and  $X_p \approx 1/3$  one obtains  $\dot{E}_{\text{osc}}/\dot{E} = 1.64$ . However this is only approximate. In practice one has to also account for the rate of energy loss due to radiation and incorporating all these a detail numerical simulation shows a 60% increase in the explosion energy [10].

## 2.1 Parameters for complete MSW flavour conversion of neutrinos

Neutrino flavor evolution in supernovae has been discussed in detail in [10, 11, 12]. Here we give the basic equations needed for our purpose. We confine our discussions to two neutrino flavors and take these to be  $\nu_e$  and  $\nu_\tau$ . The mass matrix  $M_F^2$  (see eq.(3.4)) in flavor basis for this case is

$$M_F^2 = U \begin{pmatrix} 0 & 0 \\ 0 & \Delta \end{pmatrix} U^\dagger + \begin{pmatrix} V_{cc} & 0 \\ 0 & 0 \end{pmatrix} + \begin{pmatrix} V_{nc} & 0 \\ 0 & V_{nc} \end{pmatrix} + \begin{pmatrix} V_{\nu_e \nu_e} & V_{\nu_e \nu_\tau} \\ V_{\nu_\tau \nu_e} & V_{\nu_\tau \nu_\tau} \end{pmatrix} \quad (6)$$

$V_{cc}$  is due to charged current  $\nu_e - e$  scattering and is given by  $\sqrt{2}G_F n_e E$ ,  $n_e$  is the net electron density.  $V_{nc}$  is due to neutral current scattering off neutrons and nuclei. This is identical for both flavors and can be discarded. The last piece in (6) is due to neutrino-neutrino exchange scattering. It has been shown in [12] that this term has

negligible effect on the adiabatic transitions important for the shock-reheating epoch and in what follows we will neglect this contribution. By equating the two diagonal elements of the remaining terms in (6) one arrives at the following resonance condition [10],

$$\rho_{\text{res}} = (6.616 \times 10^6 \text{g/cc}) \left( \frac{\cos 2\theta_V}{Y_e} \right) \left( \frac{\Delta m^2}{\text{eV}^2} \right) \left( \frac{1 \text{MeV}}{E_\nu} \right) \quad (7)$$

The effectiveness of neutrino oscillations in increasing the heating rate depends very crucially on whether a resonance is encountered between the neutrino-sphere and the shock front or not. If a neutrino of flavor  $f$  encounters a resonance between the neutrino-sphere and the shock then its probability to remain a  $\nu_f$  at the position of the shock is given as,

$$P(\nu_f \rightarrow \nu_f) = 0.5 + (0.5 - P_J) \cos 2\theta_{R_\nu} \cos 2\theta_{R_m} \quad (8)$$

where  $\theta_{R_\nu}$  ( $\theta_{R_m}$ ) is the neutrino mixing angle in matter at the position of the neutrino-sphere (shock) and can be expressed as,

$$\tan 2\theta_{R_i} = \tan 2\theta_V / (1 - \rho_{R_i} / \rho_{\text{res}}) \quad (9)$$

where  $R_i$  can be  $R_\nu$  or  $R_m$ .  $E_\nu$  is the neutrino energy;  $P_J$  is the non-adiabatic transition probability between the two neutrino states and can be expressed in the Landau-Zener approximation as,

$$P_J = \exp(-E_{NA}/E_\nu) \quad (10)$$

where,

$$E_{NA} = \frac{\pi}{2} \left( \frac{\sin^2 2\theta_V}{\cos 2\theta_V} \right) \frac{\Delta m^2}{\left( \frac{1}{n_e} \frac{dn_e}{dr} \right)_{\text{res}}} \quad (11)$$

A neutrino passing through the resonance density can undergo complete flavor transformation for appropriate values of the parameters. A total conversion of the  $\nu_\tau$ , which carry a higher energy, to  $\nu_e$  between the neutrino-sphere and the shock will generate maximum heating. In the region between the neutrino-sphere and the shock the neutrinos pass through a decreasing density profile. For fixed values of  $\Delta m^2/E$  and  $\theta_V$ , (7) allows one to determine the resonance density. Since we are interested in complete

conversion we have to ensure that not only is a resonance attained, but  $P(\nu_f \rightarrow \nu_f)$  as given by (8) is zero. Following situations might arise:

- $\rho_{\text{res}} > \rho_{R_\nu} > \rho_{R_m}$ , which implies that resonance position is below the neutrino-sphere. No resonance is achieved by the neutrinos coming from the neutrino-sphere and hence the probability of level-jumping at resonance  $P_J$  is zero in the region between the neutrino-sphere and the shock. Considering the limiting case of  $\rho_{\text{res}} \gg \rho_{R_\nu}$ , (9) implies  $\theta_{R_\nu} \rightarrow \theta_V$ . Also,  $\rho_\nu \ll \rho_{R_m}$  and  $\theta_{R_m} \rightarrow \theta_V$ . Then from (8),  $P_{\nu_f \nu_f} \rightarrow \frac{1}{2}(1 + \cos^2 2\theta_V)$ . The maximum conversion that one can obtain is therefore 0.5 when  $\cos 2\theta_V \approx 0$ .
- $\rho_{\text{res}} < \rho_{R_m} < \rho_{R_\nu}$ , which implies a resonance position outside the shock and again  $P_J$  would be 0. In the limit  $\rho_{\text{res}} \ll \rho_{R_m}$ , This case corresponds to  $\theta_{R_m} \rightarrow \pi/2$ .  $\theta_{R_\nu} \rightarrow \pi/2$  as well so that from (8),  $P_{\nu_f \nu_f} \rightarrow 1$ . Thus in this situation complete conversion is not a possibility.
- $\rho_{R_\nu} \geq \rho_{\text{res}} \geq \rho_{R_m}$ , which implies a resonance is met between the neutrino-sphere and the shock. The limiting case  $\rho_{\text{res}} \ll \rho_{R_\nu}$  implies  $\theta_{R_\nu} \rightarrow \pi/2$ . On the other hand in the limit  $\rho_{\text{res}} \gg \rho_{R_m}$  corresponds  $\theta_{R_m} \rightarrow \theta_V$  so that (8) becomes  $0.5 - (0.5 - P_J) \cos 2\theta_V$ . For small  $\theta_V$ ,  $\cos 2\theta_V \rightarrow 1$  and  $P_{\nu_f \nu_f} \approx P_J$ . Complete conversion can be obtained if  $P_J$  is zero *i.e.* transitions are adiabatic. If on the other hand  $\theta_V$  is large and  $\cos 2\theta_V$  is 0,  $P_{\nu_f \nu_f} \approx 0.5$  and complete conversion is not possible.

Thus complete conversion is possible only in the last situation discussed above which requires  $\rho_{R_\nu} \geq \rho_{\text{res}} \geq \rho_{R_m}$ . This gives the following constraint on  $\Delta m^2$  for  $\cos 2\theta_V \approx 1$ ,

$$(5.6 \times 10^{-8} \text{ eV}^2) \left( \frac{E_\nu}{\text{MeV}} \right) \left( \frac{\rho_{R_m}}{\text{g/cm}^3} \right) \leq \Delta m^2 \leq (5.6 \times 10^{-8} \text{ eV}^2) \left( \frac{E_\nu}{\text{MeV}} \right) \left( \frac{\rho_{R_\nu}}{\text{g/cm}^3} \right) \quad (12)$$

where we have taken  $Y_e = 0.37$ . For typical values of the densities and energies this gives  $\Delta m^2 \sim 100 - 10^4 \text{ eV}^2$  which is in the cosmologically interesting range.

Complete flavor conversion occurs when transitions are adiabatic. From the validity of the adiabatic condition,  $E_{NA} \geq E_\nu$  a lower bound on  $\theta_V$  can be obtained

$$\frac{\sin^2 2\theta_V}{\cos 2\theta_V} \geq 1.258 \times 10^{-4} \left( \frac{\text{eV}^2}{\Delta m^2} \right) \left( \frac{(\frac{1}{n_e} \frac{dn_e}{dr})_{\text{res}}}{\text{km}^{-1}} \right) \left( \frac{E_\nu}{\text{MeV}} \right) \quad (13)$$

Taking some typical values  $\Delta m^2 \sim 1600 \text{ eV}^2$  and the density scale height  $dl n n_e / dr \sim 50 \text{ km}$  one gets

$$\sin^2 2\theta_V \geq 10^{-8} \frac{E_\nu}{10 \text{ MeV}}. \quad (14)$$

In fig. 1 we give an illustrative plot taking a density profile [1]  $\rho = (10^{31} \text{ g/cc})(r/1 \text{ cm})^{-3}$ . It is to be noted that the actual density profile after collapse does not follow such a simple power law behaviour. The allowed regions in the  $\Delta m^2 - \sin^2 2\theta_V / \cos 2\theta_V$  plane, consistent with (99 – 100)% flavor conversion for a typical neutrino energy of 20 MeV, is shown in fig. 1. This curve is for a  $25 M_\odot$  star with the shock positioned at the minimum distance from the neutrino-sphere 190 km since at this position most stringent constraints on the parameters are obtained [13].

### 3 r-process nucleosynthesis

Heavy neutron rich nuclei beyond the iron group are synthesised by neutron capture. There are two basic processes:

- **s-process** or slow process for which the time of neutron capture  $t(n, \gamma) \gg t_\beta$ , where  $t_\beta$  is the beta decay life time. Thus nuclides are built along the stability valley.
- **r-process** or rapid process for which  $t(n, \gamma) \ll t_\beta$  and very neutron rich unstable nuclei are built. The above condition requires a neutron density  $n_n > 10^{19} \text{ cm}^{-3}$ .

Many authors conjectured that type-II supernovae can be a possible site for r-process nucleosynthesis since it has the required high neutron number densities  $> 10^{20} \text{ cm}^{-3}$ , temperatures  $\sim 2 - 3 \times 10^9 \text{ K}$  and time scales  $\sim 1 \text{ s}$  [14]. But where exactly in the



supernova does the r-process actually take place is a debatable issue. In the recent years the neutrino heated ejecta from the post core bounce environment of a type II supernova or the “hot bubble” has been suggested as a site for r-process [15, 16]. The “hot bubble” is the region between a protoneutron star and the escaping shock wave in a core-collapse supernova. The material in this region has a low density because of the successful explosion and yet very hot  $\sim 10^9$ K. The shock reheating epoch is between  $\sim 0.1 - 0.6$  s after core bounce whereas the r-process epoch is  $\sim 3 - 20$  s after core bounce. The major advantage which the “hot bubble” has over other proposed sites is that it correctly predicts that only  $10^{-4}M_\odot$  of r-process nuclei are ejected per supernova [17]. The late time ( $t_{pb}= 3 - 15$ s) evolution of  $20M_\odot$  delayed SN explosion model gives an excellent fit to the solar r-process abundance distribution [16].

For r-process to take place in supernova neutron rich conditions are needed. This in turn requires that the electron fraction  $Y_e$  defined as

$$Y_e = \frac{\text{No. of electrons}}{\text{No. of Baryons}} = Y_p \quad (15)$$

be  $< 0.5$  at the weak freeze-out radius ( $r_{WFO} \sim 40 - 100$  km).  $r_{WFO}$  is defined as radius where the absorption of  $\nu_e$  and  $\bar{\nu}_e$  on free nucleons ( $\nu_e n \rightarrow e^- p$ ,  $\bar{\nu}_e p \rightarrow e^+ n$ ) freeze out and is found to be very close to the nuclear freeze-out radius in most supernova models. The expression for the value of  $Y_e$  at freeze out is given by Qian et al. [18] as

$$Y_e \approx \frac{1}{1 + \lambda_{\bar{\nu}_e p} / \lambda_{\nu_e n}} \quad (16)$$

Where  $\lambda_{\nu_e n}$  and  $\lambda_{\bar{\nu}_e p}$  are the reaction rates. The reaction rate  $\lambda_{\nu N}$ , where N can be either p or n is given by

$$\lambda_{\nu N} \approx \frac{L_\nu}{4\pi r^2} \frac{\int_0^\infty \sigma_{\nu N}(E) f_\nu(E) dE}{\int_0^\infty E f_\nu(E) dE} \quad (17)$$

where  $L_\nu$  is the neutrino luminosity (we consider identical luminosity for all the neutrino species),  $\sigma_{\nu N}$  is the reaction cross-section and  $f_\nu(E)$  is the normalised Fermi-Dirac distribution function with zero chemical potential

$$f_\nu(E) = \frac{1}{1.803 T_\nu^3} \frac{E^2}{\exp(E/T_\nu) + 1} \quad (18)$$

where  $T_\nu$  is the temperature of the particular neutrino concerned. The cross section is approximately given by [10]

$$\sigma_{\nu N} \approx 9.23 \times 10^{-44} (E/\text{MeV})^2 \text{cm}^2 \quad (19)$$

If we calculate  $\lambda_{\nu_e n}$  and  $\lambda_{\bar{\nu}_e p}$  using eq (17) then the expression for  $Y_e$  becomes

$$Y_e \approx \frac{1}{1 + T_{\bar{\nu}_e}/T_{\nu_e}} \quad (20)$$

Typical values for the neutrino temperatures when r-process is operative are [18],  $T_{\nu_e} = 3.49$  MeV,  $T_{\bar{\nu}_e} = 5.08$  MeV and  $T_{\nu_\mu} = 7.94$  MeV so that  $Y_e \approx 0.41$ . This being less than 0.5 neutron rich conditions persist in the hot bubble and r-process is possible.

### 3.1 MSW transitions and r-process

Qian *et al.* made a two flavor analysis of the matter-enhanced level crossing between  $\nu_e$  and  $\nu_\tau$  or  $\nu_\mu$ . They considered a mass spectrum in which  $m_{\nu_{\tau,\mu}} > m_{\nu_e}$  so that there is resonance between the neutrinos only and not between the antineutrinos. As a result the more energetic  $\nu_{\mu,\tau}$  ( $\langle E_{\nu_\mu} \rangle = \langle E_{\nu_\tau} \rangle \sim 25\text{MeV}$ ) get converted to  $\nu_e$  ( $\langle E_{\nu_e} \rangle \sim 11\text{MeV}$ ) increasing the average energy of the electron neutrinos. As a result of this flavour conversion the neutrino energy distribution function itself will change to (assuming two flavors)

$$f_{\nu_e}^{osc}(E) = P_{\nu_e \nu_e} f_{\nu_e}(E) + P_{\nu_\mu \nu_e} f_{\nu_\mu}(E) \quad (21)$$

But the antineutrinos do not undergo any transition in this picture so that their energy ( $\langle E_{\bar{\nu}_e} \rangle \sim 16\text{MeV}$ ) and distribution function remains the same

$$f_{\bar{\nu}_e}^{osc}(E) = f_{\bar{\nu}_e}(E) \quad (22)$$

The resonance condition is as given by eq.(7) and the mass of the  $\nu_\tau$  (or  $\nu_\mu$ ) required to undergo MSW resonance between the neutrino-sphere and the weak freeze-out radius was shown to be between 2 and 100 eV which is the right range for neutrinos to be the

hot dark matter of the Universe. The densities at the neutrino-sphere and the weak-freeze out radius is such that the matter modified mixing angle at the neutrino-sphere tends to  $\pi/2$  and that at the  $r_{WFO} \sim$  the vacuum mixing angle  $\theta_V$  so that the transition probability for small vacuum mixing angles can be approximated as

$$P_{\nu\tau\nu_e} \approx 1 - P_J \quad (23)$$

with  $P_J$  given by eqs. (10) and (11). The typical value of the density scale height is now  $\sim 0.5$  km which is two orders of magnitude smaller than the value in the shock reheating case. So that the lower limit on  $\sin^2 2\theta_V$  is about two orders of magnitude larger than it was for the shock revival scenario. The detail analysis of [18] gives the curve in fig.2. The area to the left of the curve is consistent with the  $Y_e < 0.5$  constraint required for r-process.

## 4 Neutrinos from SN1987A

From the supernova SN1987A 11 neutrino induced events were detected by the Kamiokande detector and 8 events by the IMB detector [19, 20]. These detectors are water Cerencov detectors. The dominant reaction for the detection of SN neutrinos are the charged current  $\bar{\nu}_e p \rightarrow n e^+$ .

### 4.1 $\bar{\nu}_e$ oscillation

Neutrino oscillation can modify the signal at the detector following manner

$$F(\bar{\nu}_e) = F_0(\nu_e) (1 - p) + pF_0(\bar{\nu}_\mu) \quad (24)$$

where  $F_0$  is the original spectrum and  $F$  denotes the observed spectrum. If  $p = 1$  then the detected spectrum is same as the original spectrum and if  $p < 1$  the detected  $\bar{\nu}_e$  spectrum is a mixture of the original  $\bar{\nu}_e$  and  $\bar{\nu}_\mu$  spectrum. Comparing the observed energy spectra and the expected spectra in [21] it was deduced that  $p \leq 0.35$  (99%

C.L.) depending on the assumed primary neutrino spectra. The above constraint on  $p$  can now be used to constrain the oscillation parameters.

In [21] a normal mass hierarchy ( $m_{\nu_\mu} > m_{\nu_e}$ ) between the neutrino states was considered. For this case resonance occurs between the neutrinos and not the antineutrinos. There can still be some transitions between the antineutrino states if the vacuum mixing angle is large. How much conversion is consistent with the observation is determined by the constraint on the permutation factor  $p$  and they obtained the following upper bound on the mixing angle

$$\sin^2 2\theta_V \leq \begin{cases} 0.9 & \Delta m^2 \gg 10^{-9}\text{eV}^2 \\ 0.7 & \Delta m^2 \ll 10^{-9}\text{eV}^2 \end{cases}$$

Thus the vacuum oscillation solution and partly the large mixing MSW solution to the solar neutrino problem is disfavoured. However the above bounds are sensitive to the neutrino spectrum predicted by the theoretical supernova models. In [22] certain predictions about the signal characteristics were disregarded and they arrived at the opposite conclusion that large mixing angles are actually favoured. But their conclusion is valid only for  $\Delta m^2 \leq 10^{-10}\text{eV}^2$ . In [23] a re-examination of the above has been done and they reach the same conclusion as in [21] that the solar vacuum solution is incompatible with the SN1987A data if the predicted spectrum shape is assumed to be correct.

If one takes an inverted mass hierarchy with  $m_{\nu_e} > m_{\nu_\mu}$  the  $\bar{\nu}_e - \bar{\nu}_\mu$  transitions are resonant and there is a large amount of conversion inconsistent with observation. A large range of mass and mixing parameters

$$\begin{aligned} 10^{-8} &\leq \Delta m^2 \leq 10^4 \\ 10^{-8} &\leq \sin^2 2\theta_V \leq 1 \end{aligned}$$

are thus excluded for an inverted mass scheme from SN1987A observations.

## 4.2 $\nu_e$ oscillation

Since the first event in Kamiokande shows forward peaking there was a speculation that it might come from  $\nu_e - e$  scattering and many authors discussed the impact of matter-induced oscillation on the basis of this [24] and a large range of mass and mixing angles can be shown to be disfavoured. However because these analyses are based on a single event the statistical significance is questionable.

Haxton in 1987 pointed out that the reaction  ${}^{16}\text{O}(\nu_e, e)F^{16}$  cross-section increases very sharply with energy [25]. Thus this reaction which occurs in the water Cerencov detectors can be very sensitive to neutrino flavour conversion as the  $\nu_e$ s coming from flavour converted  $\nu_\mu$ s or  $\nu_\tau$ s will have higher energy. In [26] the effect of matter enhanced neutrino conversion on these events was examined. They showed that in KII if the  $P_{\nu_e\nu_e}$  is 1 corresponding to no oscillation the number of oxygen events are 7 whereas for complete conversion ( $P_{\nu_e\nu_e}=0$ ) the number of events increase to 32. They showed that a mass spectrum which is consistent with the constraints of r-process nucleosynthesis in SN and the solar neutrino problem:  $\Delta_{13} \approx 1 - 10^4 \text{eV}^2$  and  $\sin^2 2\theta_{13} = 4 \times 10^{-6}$  and  $\Delta_{12} \approx 10^{-6} - 10^{-5} \text{eV}^2$  and  $\sin^2 2\theta_{12}$  in the non-adiabatic solar range can give a large conversion probability. This mass spectrum gives two well separated resonances in the supernova.

## 5 Future Detectors

The next generation solar neutrino detectors like SNO or Super-Kamiokande can also be used to detect neutrinos from a nearby supernova explosion. SK is a 32 kt water cerencov detector. The dominant detection reaction is capture of  $\bar{\nu}_e$  on protons. SNO is a heavy water detector made of 1 kton of pure  $\text{D}_2\text{O}$ . The main detection reactions are

$$\begin{aligned}\nu_e + d &\rightarrow p + p + e^- && \text{(CC absorption)} \\ \nu_x + d &\rightarrow p + n + \nu_x && \text{(NC dissociation)} \\ \bar{\nu}_e + d &\rightarrow n + n + e^- && \text{(CC absorption)}.\end{aligned}$$

There have been various attempts to estimate the effect of non-zero neutrino mass and mixing on the expected neutrino signal from a galactic supernova [27, 28, 26]. Burrows *et al.* [28] have considered the effect of vacuum oscillations for SNO and have found that with two-flavours the effect of vacuum oscillations on the signal is small, using their model predictions for the different  $\nu$  luminosities. Two recent works have considered the effect of two and three generation vacuum oscillation on the expected signal in SNO and Super-Kamiokande. In [29] the effect of vacuum oscillations on the neutronisation  $\nu_e$  pulse was considered [29]. This case will be discussed in [30]. In [31], the effect of flavour oscillation on the post-bounce thermal neutrino flux was considered. For the mass and mixing parameters they take two scenarios.

- **scenario 1:** Here threefold maximally mixed neutrinos with the mass spectrum  $\Delta m_{13}^2 \approx \Delta m_{23}^2 \sim 10^{-3} \text{eV}^2$  corresponding to the atmospheric range while  $\Delta m_{12}^2 \sim 10^{-11} \text{eV}^2$  in accordance with the solar neutrino problem was considered.
- **scenario 2:** Here  $\Delta m_{12}^2 \sim 10^{-18} \text{eV}^2$  for which  $\lambda \sim L$  and the oscillation effects are observable while  $\Delta m_{13}^2 \approx \Delta m_{23}^2 \sim 10^{-11} \text{eV}^2$  (solar range).

For the latter case the oscillations due to  $\Delta m_{13}^2$  and  $\Delta m_{23}^2$  are averaged out as the neutrinos travel to earth. For  $\theta_{13}$  they considered two sets of values  $\sin^2 2\theta_{13} = 1.0$  (the maximum allowed value) (case 2a) and with  $\sin^2 2\theta_{13} = 0.75$ , the best fit value from solar neutrino data (case 2b). In both these scenarios the matter effects are not important. They calculated the number of expected neutrino events from a typical type II supernova at a distance of 10kpc for the main reactions in H<sub>2</sub>O and D<sub>2</sub>O in presence and absence of oscillations [32] for the various scenarios. As a result of mixing the  $\nu_\mu$  and  $\nu_\tau$ s and the corresponding antineutrinos oscillate (with average energy  $\sim 25$  MeV) into  $\nu_e$  and  $\bar{\nu}_e$  during their passage from the supernova to the detector resulting in higher energy  $\nu_e$  and  $\bar{\nu}_e$ . Hence all the charged current events show increase in number compared to the no oscillation scenario. For the  $^{16}\text{O}$  reaction the increase is maximum (by 120 or 130%). However this is dependent on the supernova model used [33].

In conclusion, notwithstanding the various uncertainties in theoretical modeling of supernova it can be used as a good testing ground for new neutrino properties. In this article the constraints on neutrino mass and mixing are discussed from considerations of neutrino oscillation in supernova. Constraints can also be obtained on magnetic moment of neutrino in case of resonant spin-flavour transitions or on the strengths of flavour changing neutral current interactions in case of oscillations of massless neutrinos and other new neutrino properties from similar considerations.

## References

- [1] H.A. Bethe, Rev. Mod. Phys. **62**, 802 (1990); S.L. Shapiro and S.A. Teukolsky, ‘Black holes, white dwarfs, and neutron stars’, John Wiley (1983).
- [2] S.W. Bruenn, Ap. J. Suppl., **58**, 771 (1985); R.L. Bowers and J.R. Wilson, Ap. J. Suppl. **50**, 115 (1982); E.S. Myra, Phys. Rep. **163**, 127 (1988).
- [3] H.A. Bethe, G.E. Brown, J. Applegate and J.M. Lattimer, Nucl. Phys. **A324**, 487 (1979).
- [4] D.Q. Lamb and C.J. Pethik, Ap. J. **209**, L77 (1976).
- [5] J. Cooperstein *et al.*, Nucl. Phys. **A429**, 527 (1984); E.A. Baron, H.A. Bethe, G.E. Brown, *et al.*, Phys. Rev. Lett. **55**, 126 (1985); E.A. Baron, J. Cooperstein and S. Kahana, Nucl. Phys. **A440**, 744 (1985).
- [6] J.R. Wilson in ‘Numerical Astrophysics’, ed. J. Centrella, Jones and Bartlett, Boston (1985).
- [7] H.A. Bethe and J.R. Wilson, Ap. J. **295**, 14 (1985).
- [8] H.A. Bethe, Ap. J. **449**, 714 (1995).
- [9] H.T. Janka and E. Müller, Ap. J. **L109**, 448 (1995); Phys. Rep. **256**, 135 (1995); Astron. Astrophys. **306**, 167 (1996), M. Herant *et al.* Ap. J. **435**, 339 (1994).

- [10] G.M. Fuller *et al.*, ApJ. **389**, 517 (1992).
- [11] G. Sigl and G. Raffelt, Nucl. Phys. **B406**, 423 (1993).
- [12] Y.Z. Qian and G.M. Fuller, Phys. Rev. **D51**, 1479 (1995).
- [13] S. Goswami, K. Kar, A. Raychaudhuri, preprint (unpublished) (1996).
- [14] E.M. Burbidge *et al.*, Rev. Mod. Phys. **29**, 547 (1957).
- [15] S.E. Woosley and R.D. Hoffman, ApJ. **395**, 202 (1992), B.S. Meyer *et al.* ApJ. **399**, 656 (1992).
- [16] S.E. Woosley *et al.*, ApJ. **433**, 229 (1994).
- [17] G.J. Mathew and J.J. Cowan, Nature **345**, 491 (1990).
- [18] Y.Z. Qian *et al.* Phys. Rev. Lett. **71**, 1965 (1993).
- [19] K.S. Hirata *et al.* Phys. Rev. Lett. **58**, 1490 (1987) and Phys. Rev. **D38**, 448 (1988).
- [20] R.M. Bionta *et al.* Phys. Rev. Lett. **58**, 1494 (1987); C.B. Bratton *et al.*, Phys. Rev. **D37**, 3361 (1988).
- [21] A. Yu. Smirnov, D. Spergel and J.N. Bahcall, Phys. Rev. **D49**, 1389 (1994).
- [22] P.J. Kernan and L.M. Krauss, Nucl. Phys. **B437**, 243 (1995).
- [23] B. Jegerlehner, F. Neubig, G. Raffelt, Phys. Rev. **D**
- [24] J. Arafune *et al.*, Physical Rev. Lett. **59**, 1864 (1987).
- [25] W. Haxton, Phys. Rev. **D36** 2283 (1987).
- [26] Y.Z. Qian and G.M. Fuller, Phys. Rev. **D49** (1994) 1762.
- [27] E.Kh. Akhmedov and Z.G. Berezhiani, Nucl. Phys. **B373** (1992) 479.



- [28] A.S. Burrows *et al.*, Nucl. Phys. **B31** proc suppl.) (1993) 408.
- [29] D. Majumdar *et al.*, astro-ph/9807100.
- [30] D. Majumdar, the article in this issue.
- [31] S.Choubey, K.Kar, D. Majumdar, hep-ph/9809424, (to be published in Journal of Physics G).
- [32] See Table 1 of [31].
- [33] In [31] the model from T. Totani *et al.*, Astrophys. J. **496** (1998) 216 is used.

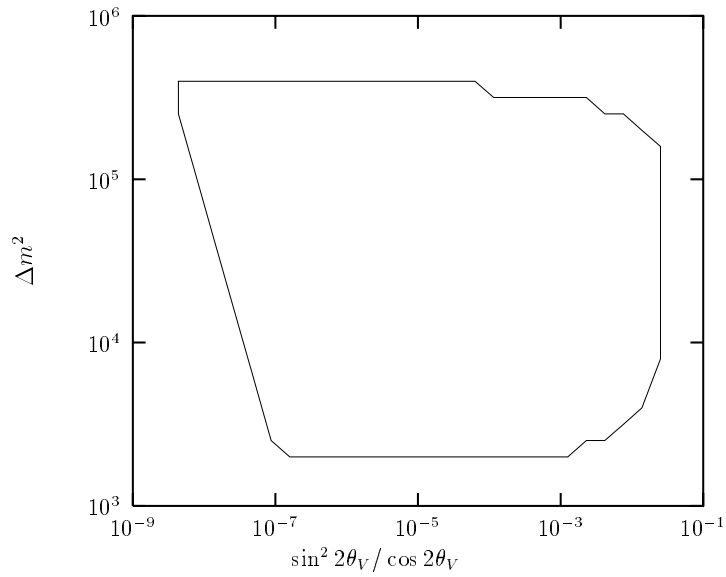


Figure 1: The allowed area in the  $\Delta m^2$  vs.  $\sin^2 2\theta_V / \cos 2\theta_V$  plane that gives complete conversion in a  $25M_\odot$  star.

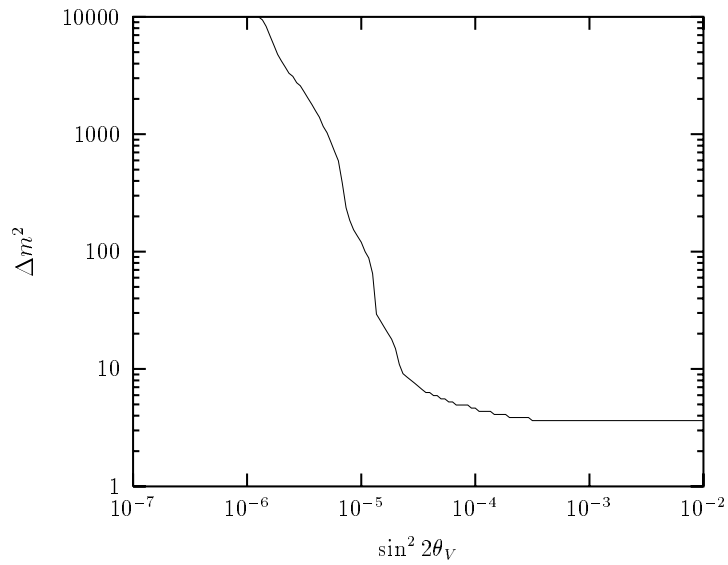


Figure 2: The allowed area consistent with the  $Y_e < 0.5$  constraint is to the left of the solid curve.